Microfluidics and Nanofluidics (2023) 27:26
https://doi.org/10.1007/s10404-023-02637-4

RESEARCH PAPER

Experimental and numerical study on air-to-nanofluid thermoelectric cooling system using novel surface-modified Fe_3O_4 nanoparticles

Faraz Afshari[1] · Emre Mandev[1] · Shabnam Rahimpour[2] · Burak Muratçobanoğlu[1] · Bayram Şahin[3] · Eyüphan Manay[1] · Reza Teimuri-Mofrad[2]

Received: 19 June 2022 / Accepted: 2 March 2023 / Published online: 23 March 2023

Abstract

Peltier cooling systems are usually smaller, more portable, and relatively simpler to operate compared to conventional vapor compression cooling systems. For this reason, Peltier cooling systems are widely recommended for use in the field of cooling applications and refrigerators. These cooling systems have relatively low efficiency despite extensive operation. To solve this problem, a Peltier cooling system operated with advanced nanofluid is proposed in this study. In this cooling system, water-based Fe_3O_4 nanofluids were used to cool the Peltier. In order to obtain high stability in these nanofluids, the nanoparticles were synthesized chemically with surface modification processes ($Fe_3O_4@SiO_2@(CH_2)_3IM$). By designing and manufacturing an air-to-nanofluid cooling system, the performance of Peltier cooling system was evaluated and compared to the conventional air-to-water system. The nanofluids were prepared in three different volume concentrations as 0.2%, 0.5% and 1.0% and then were examined at different working conditions. This research has been analyzed using both experimental and numerical methods. Temperature measurements and experimental COP evaluations were made in the cooling chamber. The flow structure and temperature distribution in spiral heat exchanger were closely surveyed and discussed in detail. According to the results obtained, nanofluid volumetric concentrations, inlet temperatures and mass flow rates had a significant effect on the cooling performance of the Peltier systems. It was observed that COP values decreased over time in all experiments and approach zero gradually.

Keywords Nanofluid · Cooling systems · Thermoelectric · COP · Heat exchanger · Fe_3O_4

List of symbols

CFD	Computational fluid dynamics
COP	Coefficient of performance
C_p	Specific heat capacity (J/kg.K)
C_μ	Turbulence constant
I	Electrical current (A)
k	Thermal conductivity (W/m.K)
K	Device thermal conductance (W/K)
m	Mass (kg)
NF	Nanofluid
NP	Nanoparticle
P	Pressure (Pa)
Q	Heat transfer (J)
R	Electrical resistance (Ω)
T	Temperature (°C)
t	Time (s)
TE	Thermoelectric
TEC	Thermoelectric cooler
V	Voltage (V)
v	Air velocity (m/s)
WBT	Water bath temperature °C
W	Power consumption (J)
∀	Volume (m^3)
ρ	Density (kg/m)
φ	Volume fraction
ϵ	Turbulent dissipation rate (m^2/s^3)
μ	Dynamic viscosity (kg/m.s)
μ_t	Turbulent viscosity (kg/m.s)
α	Seebeck coefficient (V/K)

✉ Faraz Afshari
faraz.afshari@erzurum.edu.tr

✉ Reza Teimuri-Mofrad
teymouri@tabrizu.ac.ir

[1] Department of Mechanical Engineering, Erzurum Technical University, Erzurum, Turkey

[2] Faculty of Chemistry, Department of Organic and Biochemistry, University of Tabriz, Tabriz, Iran

[3] Department of Mechanical Engineering, Istanbul Technical University, Istanbul, Turkey

Subscripts

∞	Free stream or ambient
a	Air
bf	Base fluid
c	Cold side
fa	Fan
h	Hot side
m	Mean
max	Maximum
nf	Nanofluid
p	Particle
pe	Peltier
pu	Pump
tot	Total

1 Introduction

Globally, a significant section of electrical energy is used for cooling and long-term preservation of food, medicine, etc. products. In accordance with this purpose, vapor compression systems are widely utilized. However, many researchers are working on thermoelectric systems that can be used for the same purpose as vapor compression systems. Nowadays, with the increase in energy consumption, the use of high-efficiency vehicles is gaining more importance. Although the efficiency of thermoelectric systems is not as much as the conventionally used vapor compression systems, they are advantageous because they do not have extra costs, such as valves, compressors, and working fluids (Pourkiaei et al. 2019; Afshari et al. 2020). In the studies carried out on the thermoelectric cooler, various methods are applied to throw away the heat from the cooler to the ambient. The most common of these methods are air to a refrigerant fluid (Gökçek and Şahin 2017), air-to-air with forced convection through a fan (Çağlar 2018), or air-to-air with natural convection (He et al. 2021).

Although air-to-air systems are quieter and require less equipment, it has been determined by experimental studies that their cooling performance is lower than air-to-liquid systems (Afshari 2021). For this reason, it may be more convenient to use liquid to remove waste heat in thermoelectric cooling systems. An air-to-water thermoelectric system prototype was designed and produced by Afshari (Afshari 2020) and the efficiency of the system in heating and cooling modes was compared. The Coefficient of Performance (COP) value was approximately 200% higher in the heating mode than in the cooling mode after 60 s. Additionally, it was stated that the energy consumption was higher in cooling mode. In another study, experiments were carried out by placing Peltier modules in an air channel and integrating a water-cooling system on the modules to remove heat. The COP values obtained with this installed system were found to be slightly more than 1.5 in the cooling mode and almost 2 in the heating mode (Cosnier et al. 2008). A thermoelectric system providing air-to-water cooling was developed by Tan and Zhao (Tan and Zhao 2015) and the effect of the phase changer on the system performance was investigated by integrating a phase change material into this system. The experiments performed have demonstrated that the phase change material increases the COP value of the system by 56%. In a study, tests were carried out on a thermoelectric cooler integrated with a mini-channel heat exchanger by Chein and Chen (Chein and Chen 2005). It has been reported that the internal temperature of the cooler can decrease with the increase of the applied electric current and the decrease of the thermal resistance of the heat sink.

It has been proven by many studies in this field that nanofluids exhibit better thermal performance than conventional fluids, such as water, ethylene, and oil (Huminic and Huminic 2011; Tiwari et al. 2013; Zheng et al. 2020; Kumar and Sonawane 2016; Yu et al. 2008; Bhatti et al. 2022; Özerinç et al. 2010). Since the thermal conductivity of solids is quite high compared to liquids and nanofluids are obtained from solid particles dispersed in the liquid, the thermal conductivity of nanofluids is higher than conventional liquids. The thermal conductivity of the Al_2O_3-water nanofluid was evaluated according to the temperature and ultrasonication duration and compared with the base liquid. The maximum thermal conductivity enhancement was detected as 14.4% at 4% vol. concentration and at 65 °C temperature (Buonomo et al. 2015). In a study carried out by Esfe et.al (Esfe et al. 2015), MgO nanoparticles were dispersed in a water-ethyl glycol mixture (60:40). The maximum thermal conductivity increase compared to the base liquid approached 35% at 3% vol. Experimentally, in the study with Al_2O_3-water nanofluid, it was revealed that the heat transfer coefficient of the nanofluid was 40% higher than that of water at 6.8% vol. (Nguyen et al. 2007). The most important parameter affecting the use of nanofluids, which have positive effects in thermal applications, is their stability. The stability of nanofluids depends on many factors, such as pH values, nanoparticles concentration, size and morphology, capping agent type, and van der Waals interactions (Rahman Salari et al. 2022). The stability of nanofluids has been investigated by many researchers and optimum preparation conditions have been discussed (Liu et al. 2015; Gupta et al. 2021; Sadeghi et al. 2015).

The nanofluids used in different heat exchangers and micro/mini-channels exhibit better thermal performance than water and other conventional liquids (Asadollahi et al. 2019; Ellahi 2013) and this makes them attractive for air-to-liquid thermoelectric cooling systems. A thermoelectric system was designed and produced by Ahammed et.al (2016a) for the cooling of electronic devices. In this designed system, waste heat will be removed by transferring it to the circulating liquid in a mini-channel heat exchanger. The performances of the fluids were compared using water and 0.1 and 0.2% vol. Al_2O_3-water nanofluids as coolant. In experiments performed at various Reynolds numbers, it was determined that the COP value of the system showed a 40% improvement in 0.2% vol. nanofluid compared to water. In order to improve the performance of the thermoelectric cooling module, an experimental study was carried out using TiO_2-water and Fe_3O_4-water nanofluids. The nanofluids were obtained by dispersing 0.005% vol. TiO_2 and 0.015% vol. Fe_3O_4 nanoparticles into water. The temperature difference between the cold and hot sides of Peltier for Fe_3O_4-water nanofluid as a refrigerant is 3.94% lower than that of TiO_2 nanofluid. It was also 21.42% lower than water (Wiriyasart et al. 2021). An experimental study was conducted to examine the nanofluid effect on the cooling performance of the thermoelectric system. To achieve this aim, a water block was installed on the hot side of the Peltier module to remove the waste heat and a water-to-air heat exchanger is adapted to the system in order to throw away the heat of the liquid coming out of this block. Three different nanoparticles, SiO_2, Al_2O_3 and TiO_2, were dispersed in water at different mass fractions (0.1, 0.5 and 1%). The obtained experimental outputs indicated that the Al_2O_3-water nanofluid exhibited better thermal performance than the others in all cases. Considering the cooled water temperature, Al_2O_3-water nanofluid showed an increase of 55.1% compared to water (Cuce et al. 2020). In a study examining the nanofluid effect on the Peltier module, Al_2O_3-water was used as the nanofluid. In this experimental study, a heat exchanger was placed on both sides of the thermoelectric module and the performance of the system was investigated in three different situations. In these cases, the first is the use of nanofluids on both sides, the second is the use of water on the cold side and the nanofluid on the hot side, and the third is the use of nanofluid on the cold side and water on the hot side. The findings obtained in the experiments indicated that utilizing nanofluid on the hot side at low Reynolds numbers significantly increased the COP value of the system and decreased the entropy generation, but it was observed that the nanofluid on the cold side had the opposite effect (Mohammadian and Zhang 2014). In another study using nanofluid in the thermoelectric system, it was stated that graphene-water nanofluid enhanced the COP value of the system by 72% and the heat transfer coefficient by 88.62% (Ahammed et al. 2016b). In a research conducted by preparing TiO_2-water nanofluid, it was emphasized that the use of nanofluid instead of water reduces thermal resistance (Lin et al. 2020; Putra and Iskandar 2011). Another study was carried out by Nnanna et al. (Agwu Nnanna et al. 2009), water and Al_2O_3-water nanofluid were used and compared for heat disposal from the thermoelectric module. The temperature differences of the hot and cold sides of the Peltier module were assessed and the results reached illustrated that while the nanofluid was almost 0 ºC, it was higher for water.

It is seen in the literature, there is an interest in increasing the thermal performance (COP) of thermoelectric coolers with the usage of nanofluids (Maneewan et al. 2014). Although this issue has been discussed in terms of thermal performance, no evaluation has been made on nanofluid stability problems. One of the effective methods to avoid stability problems is the surface modification process. The lifetime of nanofluids can be increased by particle-specific surface modification processes. In addition, stable nanofluids can be obtained by applying surface modification to particles, such as Cu and Fe oxides, which are very difficult to prepare in the stable but show high thermal conductivity. In this study, nanofluids obtained by applying surface modification to Fe_3O_4 nanoparticles with relatively high thermal conductivity were used. The effects of the prepared long-term stable nanofluids on the thermal performance of a thermoelectric cooler were investigated. In this way, unlike the literature, a higher thermal performance increase could be achieved and a thermal system design with a long service life was proposed. Air-to-nanofluid Peltier cooling system has been designed and manufactured to improve the efficiency of the cooling system using stable Fe_3O_4-water nanofluid in different volume concentrations. The used heat exchanger was also simulated using ANSYS Fluent as a CFD program.

2 Experimental procedure details

2.1 Preparation of $Fe_3O_4@SiO_2@(CH_2)_3IM$ NPs

The $Fe_3O_4@SiO_2@(CH_2)_3IM$ NPs were synthesized according to published method presented in open literature (Teimuri-Mofrad et al. 2018a, b). Briefly, $FeCl_2$, $4H_2O$ and $FeCl_3$ were heated in deionized water to 80 °C and NH_4OH was added to the stirred solution. The observed precipitates are Fe_3O_4 NPs which collected by an external magnet, washed with deionized water, and dried in the oven at 60 °C. The Fe_3O_4 NPs were dispersed in EtOH and deionized water, NH_4OH along with 2 mL tetraethyl orthosilicate were added at 50 °C. After 2 h $Fe_3O_4@SiO_2$ precipitates were separated by the magnet. In continue, the $Fe_3O_4@SiO_2$ were dispersed in toluene and (3-chloropropyl) trimethoxysilane was added and stirred for 24 h. Then, N-methylimidazole was added and mechanically stirred for 48 h. The $Fe_3O_4@SiO_2@(CH_2)_3IM$ was separated by magnet, and dried by the oven. In order to approve the nano-sized dimensions of prepared $Fe_3O_4@SiO_2@(CH_2)_3IM$ NPs, the SEM image was displayed in Fig. 1. Spherical morphology with an

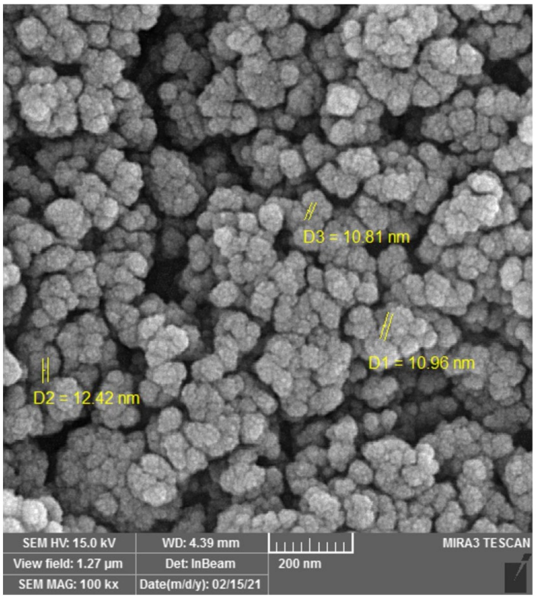

Fig. 1 SEM image of Fe_3O_4@SiO_2@$(CH_2)_3$IM NPs

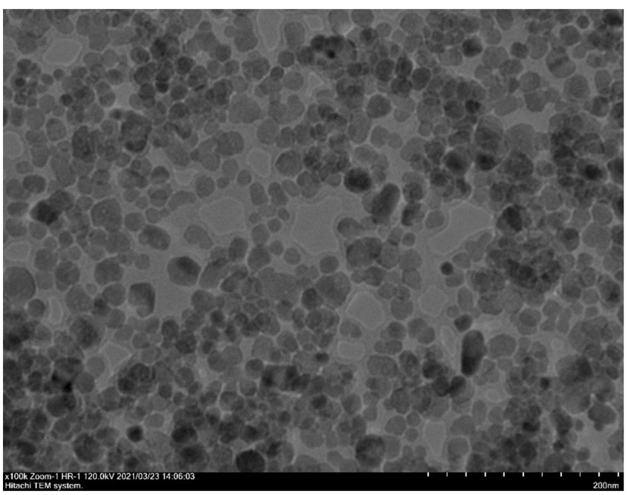

Fig. 2 TEM images of Fe_3O_4@SiO_2@$(CH_2)_3$IM NPs

average diameter of about 12 nm for prepared NPs were observed.

The Fe_3O_4@SiO_2@$(CH_2)_3$IM NPs were also characterized via transmission electron microscopy (TEM) technique (Fig. 2). The TEM image demonstrated the spherical shape as well as the core–shell structure of the synthesized nanoparticle.

2.2 Preparation of nanofluid

In this section, total amounts of pure water and nanoparticles required for the preparation of nanofluids with volume concentration ratios of 0.2%, 0.5%, and 1% were calculated. As shown in the schematic view below (Fig. 3), the mixture of pure water and nanoparticles was initially prepared and then mechanically stirred. Finally, a Hielscher UP400S ultrasonic homogenizer device was used to prepare a homogeneous nanofluid. The homogenizer was operated with a power of 200 W at 10 kHz for 210 min. The anti-decomposition properties of nanofluids prepared with surface-modified nanoparticles were evaluated in detail by Mandev et al. (2022). In this study, the long-term stability and thermo-physical property changes of nanofluid samples were investigated.

2.3 Installation of the cooling system

Peltier thermoelectric modules are a type of energy converter systems that consist of a number of semiconductors connected in series. By applying appropriate voltage, the cooling effect of thermoelectrics is revealed. In Peltier cooling systems, different kinds of heat exchangers are proposed to use on both sides to enhance heat transfer rate. In this study, a styrofoam refrigerator box with a volume of 0.0061 m^3 was utilized to examine the Peltier cooling performance. Experiments were performed on TEC1-12715 model Peltier according to the principle of air-to-water thermoelectric cooling model. After the experiments on the water system, the heat transfer fluid was replaced and nanofluids with different volume concentrations were used, which was named as air-to-nanofluid cooling model. In the hot side of Peltier module, a liquid-cooled exchanger was used (Al heat exchanger). In this heat exchanger, fluid temperature rises and this temperature should be decreased to the requested inlet temperature. For this reason, fluid was transferred to the fluid tank by passing through the spiral heat exchanger in the constant temperature water bath. On the cold side, a small fan and heat exchanger have been employed. The pump, Peltier and cooling chamber fan used in the system were supplied with a multi-channel DC power supply. A schematic view of the installed setup is given in Fig. 4 in more detail.

The temperature of cooling chamber was measured using four K-type thermocouples and a data logger during the test time. The obtained data was transferred to a computer using a Hioki LR8402-20 model data logger with 0.01 ℃ resolution. In the calculations, average values of obtained temperatures were computed and used as the mean temperature of the cooling chamber. The properties of the used Peltier module and water pump are presented in Table 1. In this work, the temperature variation of the cooling chamber was also evaluated by a TESTO 885-2 model thermal Imager, which accuracy and thermal sensitivity are ± 2 °C and < 30 mK at 30 °C, respectively. In Table 2, various parameters performed in the experiments have been presented.

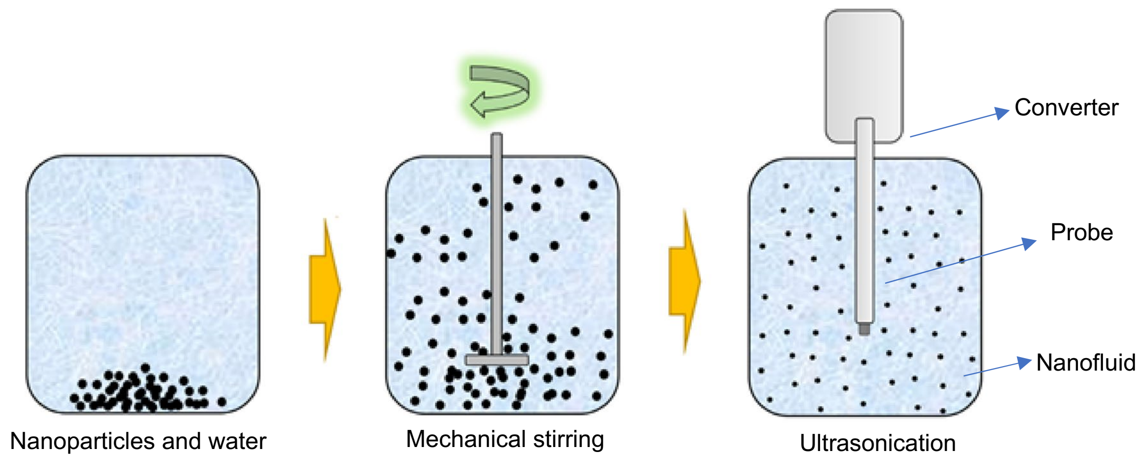

Fig. 3 The process of preparation nanofluids

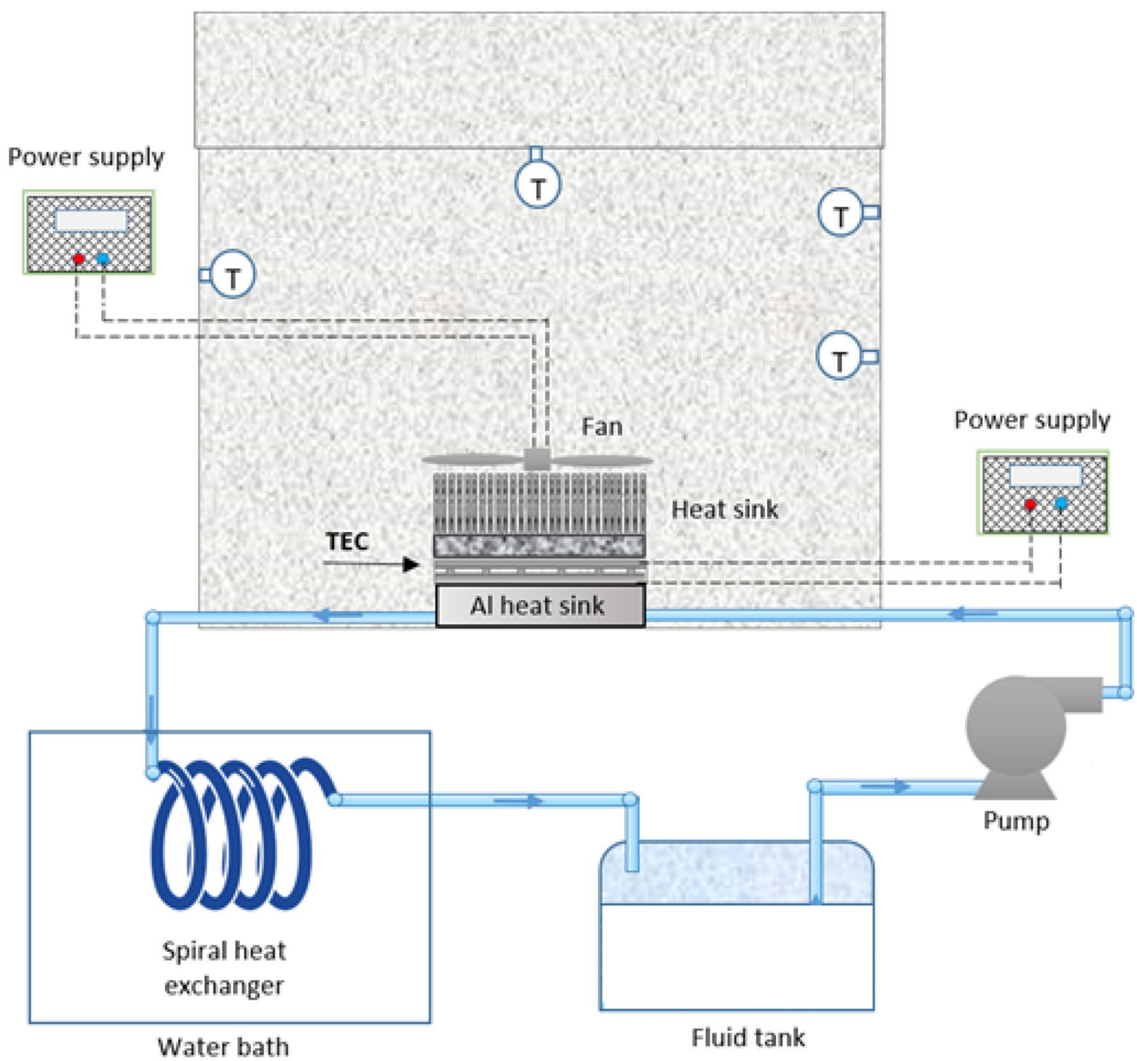

Fig. 4 Schematic view of the installed cooling system

Table 1 Properties of used Peltier module and water pump

Peltier module						
Model	Operating voltage	Operating current	I_{max}	Dimensions	Q_{max}	
TEC1-12715	12 V	<3 A	15 A	4×4×0.4 cm	231 W	
Water pump						
Model	Operating voltage	Motor type	Flow rate	Dimensions	Working temperature	Weight
Kamoer NKP DCL	DC-12 V	Permanent magnet	10–60 ml/min	41×55×67 mm	0–50 °C	0.2 kg

Table 2 Various parameters selected in the experiments

Volume concentration	Water bath temperatures	Mass flow rates
Pure water	5 °C	0.0003 kg/s
0.2% vol. NF	10 °C	0.0006 kg/s
0.5% vol. NF	15 °C	0.0009 kg/s
1.0% vol. NF	20 °C	0.0012 kg/s
–	–	0.0015 kg/s

3 Numerical approach

In this section, the spiral-type heat exchanger used for cooling nanofluids was simulated by CFD methods. The geometry of heat exchanger was created in Fluent software and the mesh generation was performed, then boundary conditions of the domain were defined. The working conditions selected in the experimental analyses were considered in numerical solutions to evaluate temperature distribution and flow structure in spiral heat exchanger. In Fig. 5, the geometry and boundary condition of the spiral heat exchanger are presented.

In the simulation created, it was assumed that the thermo-physical properties of the fluid do not change with temperature. In addition, solutions were made considering steady-state conditions. Parallel solver was selected in Fluent launcher settings. Since there is an incompressible flow in the simulation performed, the solvent type was preferred pressure-based. Also, the velocity formulation was determined as absolute. In order to obtain more precise results, couple was chosen in the scheme section of the solution method. Direct Numerical Simulation (DNS) method is generally insufficient to simulate the flow field and vortices. Therefore, Reynolds-Averaged Navier-Stokes (RANS) equations have been used in this simulation (Afshari et al. 2022a). In addition to all these, turbulent kinetic energy and turbulent dissipation rate were chosen as first order upwind and momentum and energy equations were chosen as second order upwind.

The walls of water bath are in constant temperatures during test time. In the next figures, the configuration of mesh generated for spiral heat exchanger and whole system are illustrated (Fig. 6). With the aim of having the required accuracy, several revisions and different mesh numbers and configurations have been considered to solve the problem with minimum error rate. For this purpose, the MultiZone method was applied to obtain a smooth mesh configuration on the spiral heat exchanger. Since there is no flow in the enclosure area, no method has been applied to facilitate the solution. It should be stated in the regions near walls and boundaries a more compact and finer mesh were applied. Additionally, the skewness value of produced meshes was

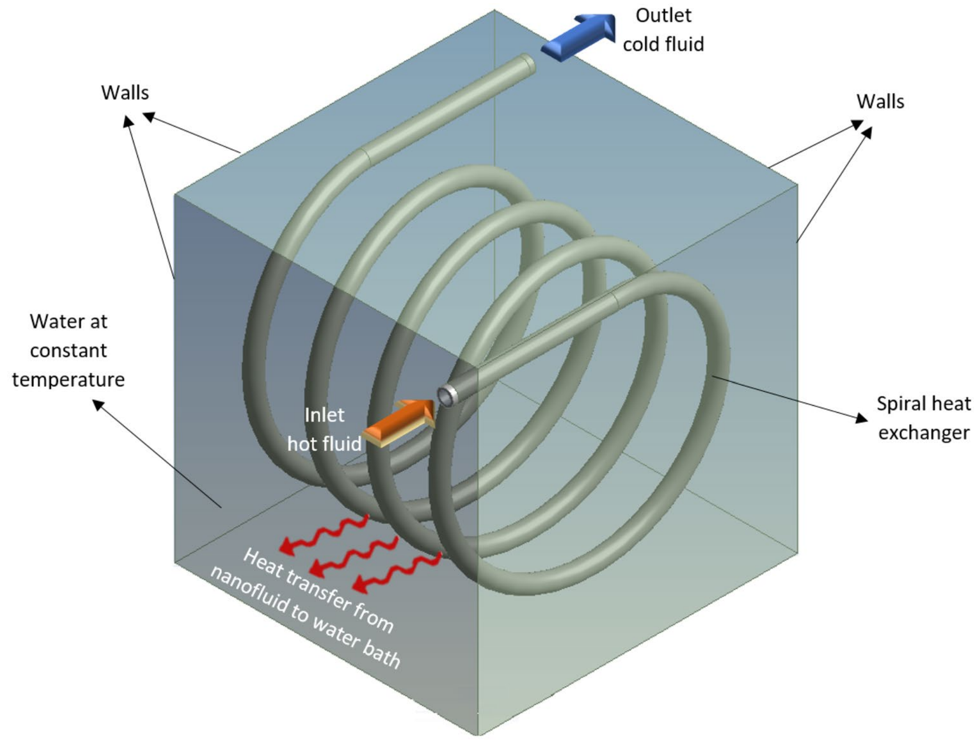

Fig. 5 Geometry and boundary condition defined domain spiral heat exchanger

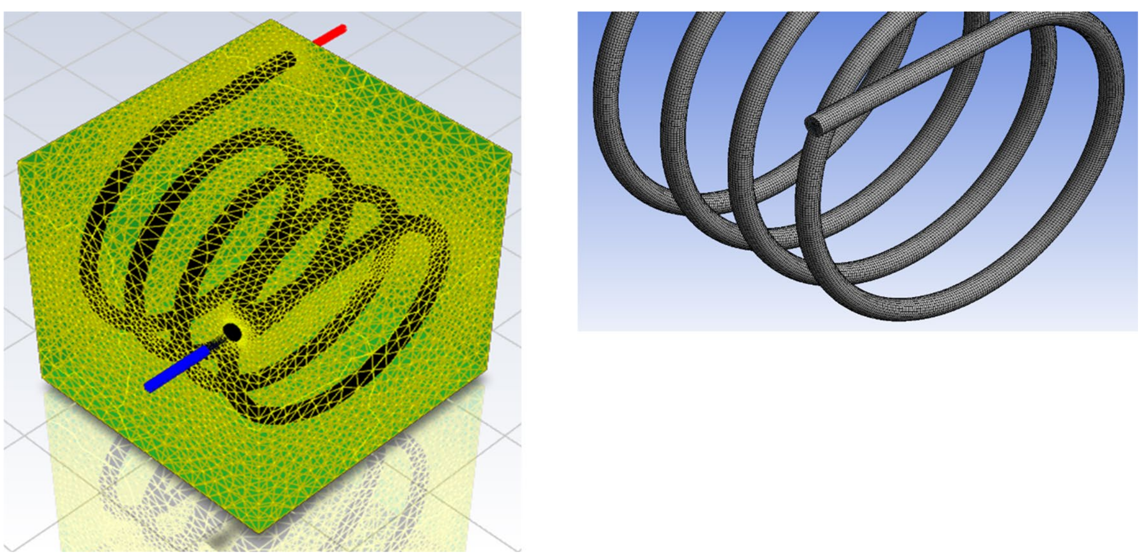

Fig. 6 Mesh configuration of the spiral heat exchanger

carefully checked in numerical experiments to ensure the required precision was reached. A maximum of 1,500,000 mesh number with growth rate of 1.2 was performed in the mesh generation process. Maximum and average skewness values are 0.84 and 0.23 respectively. The average skewness values in the range of 0–0.25 indicate that excellent quality mesh is obtained (Fatchurrohman and Chia 2017; Park et al. 2022).

Computational fluid dynamics is one of the main parts of today's engineering articles, which is frequently employed for thermodynamics, aerodynamics and hydrodynamics simulation of problems. In this study, CFD analysis was also employed to evaluate the working conditions of the spiral-type heat exchanger used for cooling nanofluids. In the numerical solutions boundary conditions were defined and the governing equations were used which are given as follows (Tuncer et al. 2020, 2021; Çiftçi et al. 2021; Selimefendigil et al. 2021),

Continuity equation:

$$\nabla.\left(\rho\vec{v}\right) = 0 \quad (1)$$

Energy conservation balance:

$$\nabla.\left(\vec{V}(\rho E + p)\right) = \nabla.k_{\text{eff}}\nabla\text{T} - \text{h}\vec{J} + \left(\mu\left[\left(\nabla\vec{v} + \nabla\vec{v}^{T}\right) - \frac{2}{3}\nabla.\vec{v}I\right].\vec{v}\right) \quad (2)$$

In this equation, h represents enthalpy and $\vec{J}$ indicates diffusion flux of species.

Momentum equation:

$$\nabla.\left(\rho\vec{v}\vec{v}\right) = -\nabla p + \nabla.\left(\mu\left[\left(\nabla\vec{v} + \nabla\vec{v}^{T}\right) - \frac{2}{3}\nabla.\vec{v}I\right]\right) \quad (3)$$

In the solution, the problem was assumed to be steady state. Considering studies in the literature, k−ε Realizable method is widely utilized in CFD works (Güngör et al. 2022). In this research, the mentioned method was also utilized to solve the problem. Transport equations in k−ε model are turbulent kinetic energy (k), and rate of dissipation of kinetic energy (ε), which are expressed as,

$$\frac{\partial}{\partial x_i}\left(u_i\rho\epsilon\right) = \frac{\partial}{\partial x_j}\left[\left(\frac{\mu_t}{\sigma_\varepsilon} + \mu\right)\frac{\partial\epsilon}{\partial x_j}\right]\frac{\varepsilon}{k}G_kC_{1\varepsilon} - \rho\frac{\varepsilon^2}{k}C_{2\varepsilon} \quad (4)$$

$$\frac{\partial}{\partial x_i}\left(\left(\frac{\mu_t}{\sigma_k} + \mu\right)\frac{\partial k}{\partial x_j}\right) - \rho\varepsilon + G_k = \frac{\partial}{\partial x_i}\left[\left(u_i\rho k\right)\right] \quad (5)$$

The turbulent viscosity μ_t is obtained as;

$$\mu_t = \rho C_\mu\frac{k^2}{\varepsilon} \quad (6)$$

The turbulent kinetic energy (G_k) due to the mean velocity gradients found in Eqs. 4 and 5 is defined as;

$$G_k = -\frac{\partial u_j}{\partial x_i}\rho\overline{u_j^{'}u_i^{'}} \quad (7)$$

4 Experimental analysis and calculations

Experimental analyses were carried out to reveal performance of cooling system. In the field of cooling and heating systems, performance (COP) of the manufactured systems can be calculated using two different methods. Thermodynamically, COP value can be calculated as a ratio of cooling rate (or heating rate) to the consumed power in the system (generally is electrical power). This first method, is generally utilized in the literature, which has been also used in this work. In the following, the calculation procedure of this method has been presented. The total COP value of the Peltier cooling system can be achieved using Eq. 8. In this equation, the power consumption of electrical elements, such as water pump, fan, and Peltier module, should be taken into consideration.

$$\text{COP}_{\text{tot}} = \frac{Q_c}{W_{\text{pe}} + W_{\text{pu}} + W_{\text{fa}}} \quad (8)$$

All electrical elements have been considered and their power consumptions were calculated from the current and voltage values as,

$$W = IV \times t \quad (9)$$

Q_C is the heat energy transferred from the inside cooling chamber to the heat transfer fluid that is nanofluid in this study. For this reason, following equation was used to calculate Q_C value,

$$Q_c = mC_{\rho,a}\left(T_{m,2} - T_{m,1}\right) \quad (10)$$

In this equation, mean temperatures are the first and second average temperatures of the cooling chamber. The air mass inside cooling chamber is indicated by m, that can be obtained from volume of the cooling chamber and the density of the air as,

$$m = \rho\forall \quad (11)$$

In the second method presented in the literature, electrical properties and physical properties of the Peltier device are used to evaluate COP value of the cooling system. Assuming constant electrical and thermal features of Peltier module, cooling and heating values at cold and hot sides (Q_c and Q_h) have been expressed as,

$$Q_h = \alpha T_hI - \frac{1}{2}\left(I^2R\right) - K\left(T_h - T_c\right) \quad (12)$$

$$Q_c = \alpha T_cI - \frac{1}{2}\left(I^2R\right) - K\left(T_h - T_c\right) \quad (13)$$

and in the next step, the performance of the thermoelectric cooling system can be obtained using COP equation as follows,

$$\text{COP} = \frac{T_c}{T_h - T_c}\frac{\sqrt{1 + ZT_m} - \frac{T_h}{T_c}}{\sqrt{1 + ZT_m} + 1} \quad (14)$$

In this equation, ZT_m is defined as figure-of-merit of TE element at average cold and hot side temperatures that is T_m.

In this study, nanofluid thermo-physical properties were obtained to use in CFD simulation. Thermal conductivity and viscosity values of nanofluids were measured with the specified measuring devices (see experimental results), but density and specific heat were calculated with given equations Eqs. 15 and 16 respectively (Xuan and Roetzel 2000; Zeeshan et al. 2022).

$$\rho_{nf} = \varphi\rho_p + (1-\varphi)\rho_{bf} \tag{15}$$

$$C_{\rho,nf} = (1-\varphi)\left(\frac{\rho_{bf}}{\rho_{nf}}\right)C_{\rho,bf} + \varphi\left(\frac{\rho_p}{\rho_{nf}}\right)C_{\rho,p} \tag{16}$$

Here φ is volume concentration of nanofluid, and thermophysical properties of nanofluid are calculated using properties of both base fluid which is water in this study and particles.

5 Results and discussion

The results of experiments and CFD simulation have been presented and discussed in this section. The important parameters including temperature variation of cooling chamber, performance of the system, and heat transferred from cooling chamber (Q_c) are obtained and analyzed. Additionally, achieved results from ANSYS-Fluent modeling are given in the form of contours to evaluate temperature distribution and flow structure in the spiral heat exchanger.

5.1 Experimental results

In Figs. 7 and 8, the thermal conductivity and viscosity of nanofluid samples versus temperature were presented. In the figures, results of pure water were also presented to compare with nanofluids. It should be stated that, thermal conductivity and viscosity of pure water presented in the literature, were added to the provided diagrams.

In this context, after preparing nanofluids samples in different volume concentrations (0.2, 0.5 and 1% vol.), an A&D SV-10 model vibro viscometer and a Linseis THB 100 model thermal conductivity measuring instrument were used to obtain required data. The results presented in the figures show that, by increasing nanofluid volume

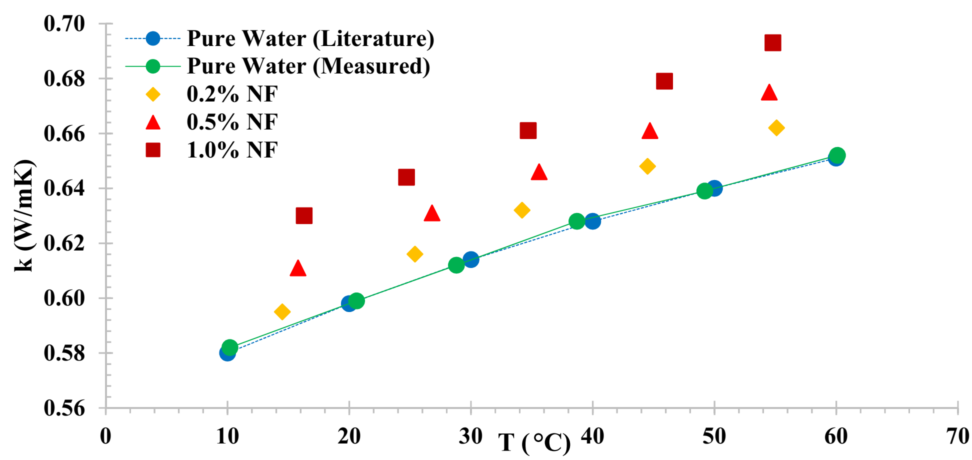

Fig. 7 Thermal conductivity of nanofluids compared to water in different temperatures

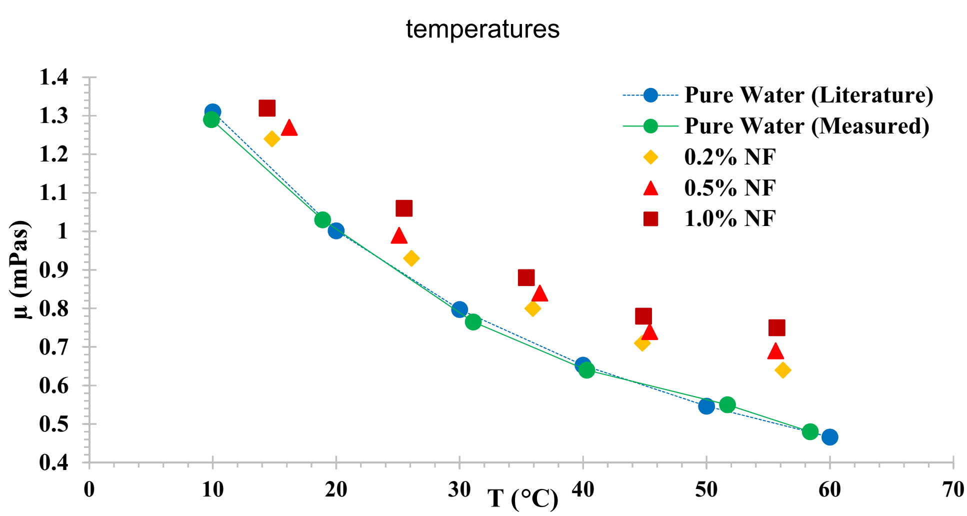

Fig. 8 Viscosity of nanofluids compared to water in different temperatures

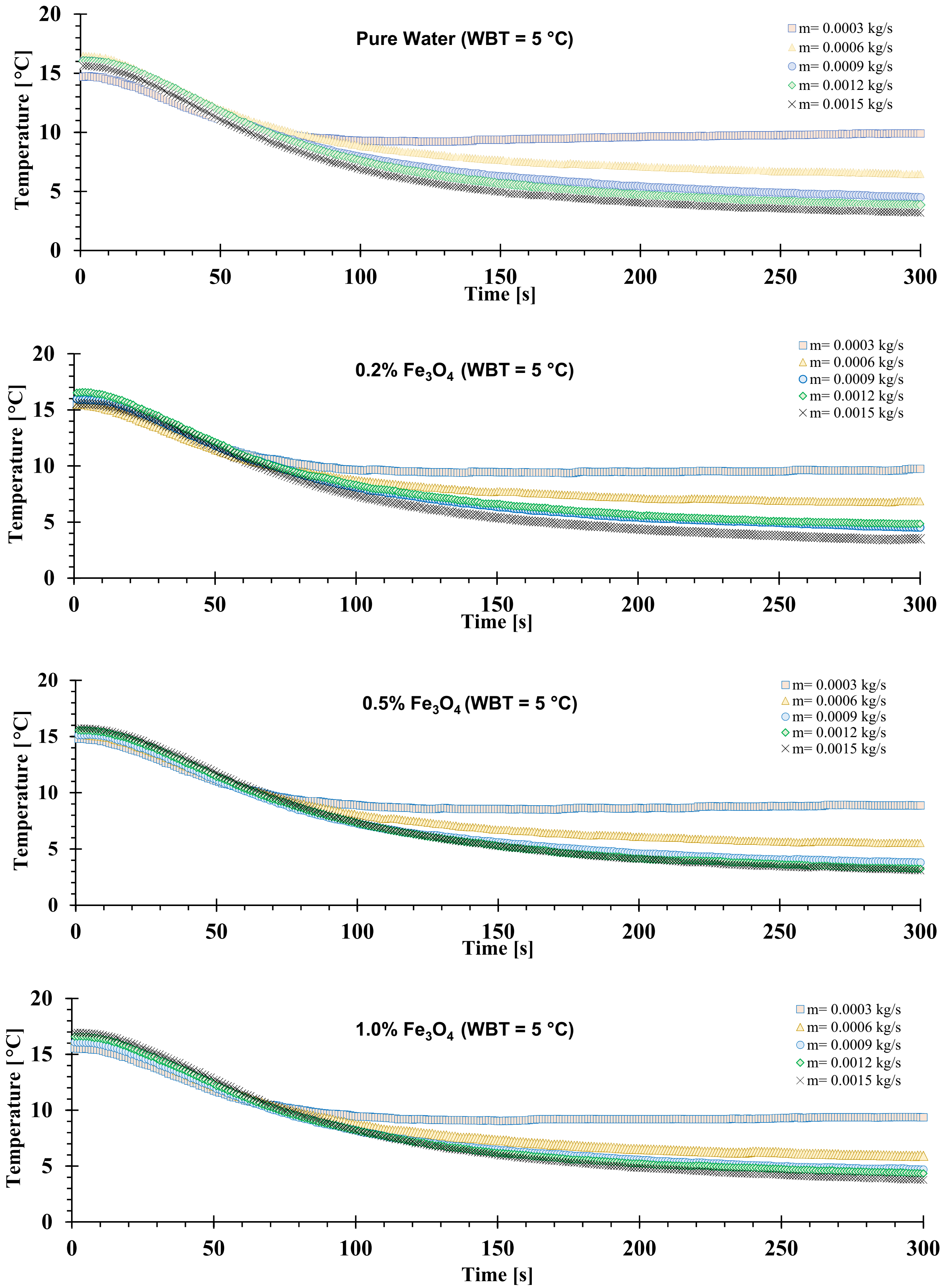
Pure Water (WBT = 5 °C)
0.2% Fe_3O_4 (WBT = 5 °C)
0.5% Fe_3O_4 (WBT = 5 °C)
1.0% Fe_3O_4 (WBT = 5 °C)
m= 0.0003 kg/s
m= 0.0006 kg/s
m= 0.0009 kg/s
m= 0.0012 kg/s
m= 0.0015 kg/s
Temperature [°C]
Time [s]
0
5
10
15
20
0
50
100
150
200
250
300

◂**Fig. 9** Temperature reduction inside cooling chamber for different heat transfer fluids (water and Fe_3O_4–water NFs (0.2%, 0.5%, and 1.0% vol.) at water bath temperature of 5 °C

concentration, both thermal conductivity and viscosity values increase and all nanofluid samples are in higher levels when compared to the pure water. Additionally, the effects of temperature on the mentioned parameters were examined. Increasing the fluid temperature increased thermal conductivity, but on the contrary, viscosity of the fluid decreased with temperature of the fluid.

Thermal conductivity increase observed in nanofluids improves thermal performance, while viscosity increase requires extra pumping power. If the fluid viscosity results given in Fig. 8 are examined, it will be seen that nanofluids have higher viscosity properties than the base fluid. The high viscosity feature also shows that the use of nanofluids will cause an increase in pumping power. In this study, no pressure loss or pump power analysis results are given directly. However, the additional pumping power was taken into account in the calculation of COP for the thermoelectric cooler given in Eq. 8.

In this part of the study, the effects of important factors including water bath temperature, mass flow rate, and used heat transfer fluid were investigated on the temperature drop of cooling chamber. In Fig. 9, temperature reduction inside cooling chamber has been presented for tested heat transfer fluids at a constant water bath temperature of 5 °C. It can be seen that, in all experiments, temperature of cooling chamber decreases with test time which is 300 s. Additionally, the mass flow rate plays a notable role in efficient cooling. The highest temperature decrease was recorded in the maximum flow rate, which is 0.0015 kg/s, and the temperature of the refrigerator approaches 3 °C.

In Fig. 10, temperature drop inside cooling chamber for different heat transfer fluids including water and nanofluids Fe_3O_4–water (0.2%, 0.5%, and 1.0% vol.) have been presented at the mass flow rate of 0.0015 kg/s. In following figures, four separate diagrams were provided to show operation conditions of different heat transfer fluids as pure water and nanofluids in different volume concentrations. In the experiments, it was observed that the effective temperature drop occurred about half of the time, but after approximately 150 s, the temperature results were fixed. At the same time, the effect of water bath temperature was clearly observed, which indicates the effective performance of spiral-type heat exchanger in the cooling apparatus. By reducing the water bath temperature from 5 °C to 20 °C in 1% volumetric nanofluid, it was observed that the temperature drop in the refrigerator at the end of the experiment changed from 8.8 °C to 3.8 °C after 300 s. This means an improvement in temperature reduction of about 5 °C.

To compare the results of using nanofluid as a heat transfer fluid, the obtained results were analyzed exactly. It was seen that the temperature drops in the cooling chamber using water and nanofluids were close to each other and the curves obtained were overlapped in the diagrams. Therefore, the results of one of the test nanofluid samples were selected and compared with the pure water. In this context, temperature reduction inside cooling chamber for nanofluid 0.5% vol. and pure water has been presented in Fig. 11. These results are presented for water bath temperatures of 5, 10, 15, and 20 °C, at mass flow rate of 0.0003 kg/s, which reveal that the nanofluid used had a relative improvement in the temperature drop of the refrigerator. As an example, at a water bath temperature of 5 °C, the temperature drops of the cooling chamber for pure water and nanofluid Fe_3O_4–water 0.5% vol., were 8.8 and 9.9 °C, respectively, which indicates an improvement of about 1 °C.

Performance value (COP) is considered as an important factor in cooling and heating systems. The apparatus that provides a high level of heating or cooling in the face of the given work has a high performance and a comparison can be made between the different energy systems considering COP value. In Fig. 12, COP results during cooling time have been presented for nanofluid sample Fe_3O_4–water (1.0% vol.) at different water bath temperatures and mass flow rates. All obtained values were taken into account and the COP values were calculated over time for all nanofluid samples. It was revealed that, the performance value initially increases in the first times of experiments but in the next stages constantly decreases over time. The reason for this can be interpreted as the reduction of the thermal energy source in the refrigerator during the test. According to this issue and in order to better compare the COP values, the average COP values for the experiments performed were calculated and presented in the following diagrams.

As noted earlier, the average results of the COP data were calculated and presented in histograms for better comparison as shown in Fig. 13. Obtained results of all tested nanofluids and water have been presented for all operating conditions. Considering the mass flow rate, it can be seen that by increasing 0.0003 kg/s to 0.0006 and 0.0009 kg/s a significant jump in efficiency results is achieved. However, with the further increase of flow rate, there has not been much change in the COP results. At the same time, the adverse effect of the water bath temperature on the performance was also clearly observed in the results. For the nanofluid sample Fe_3O_4–water (1.0% vol.), by increasing mass flow rate from 0.0003 kg/s to 0.0015 kg/s, average COP increases about 150%. When the COP values given in Fig. 13 are examined, it will be seen that the thermodynamic efficiency increases significantly with the use of nanofluid as the working fluid. For example, when the flow rate was 0.0015 kg/s and the bath temperature was 20 ºC, around 7% COP increase was

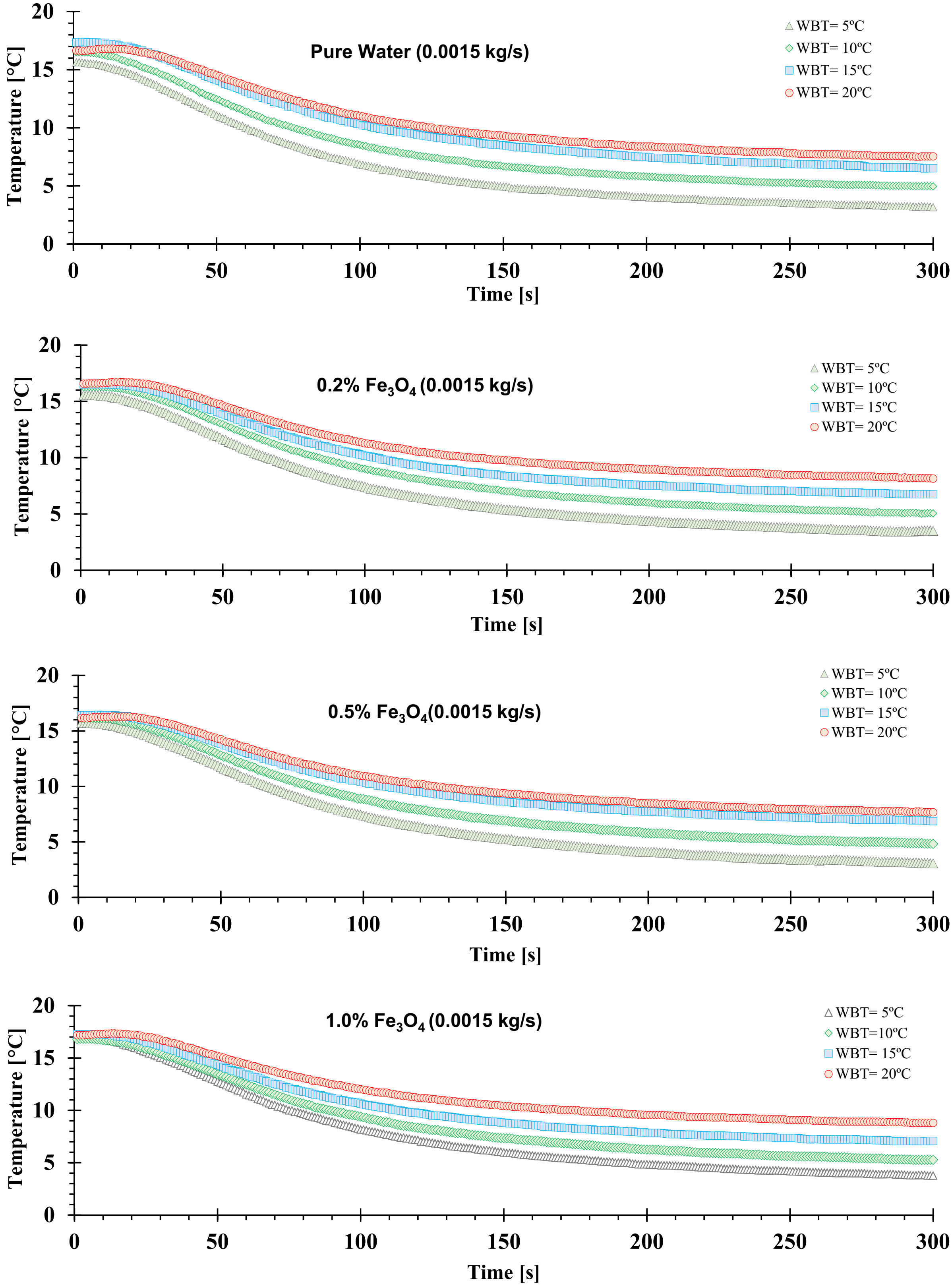

Fig. 10 Temperature reduction inside cooling chamber for different heat transfer fluids (water and Fe_3O_4–water NFs (0.2%, 0.5% and 1.0% vol.) at flow rate of 0.0015 kg/s

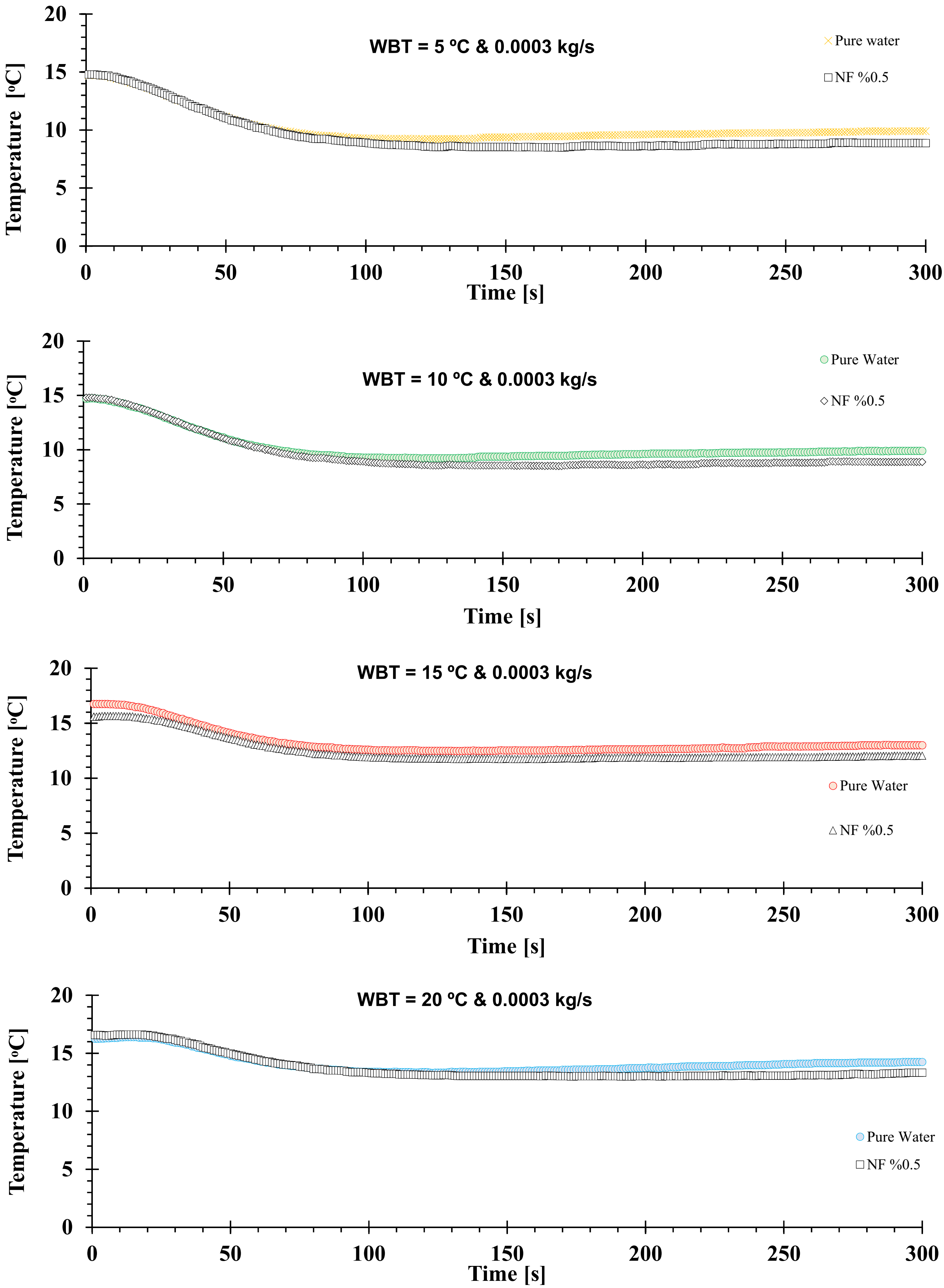

Fig. 11 Temperature reduction inside cooling chamber for pure water and nanofluid 0.5% vol

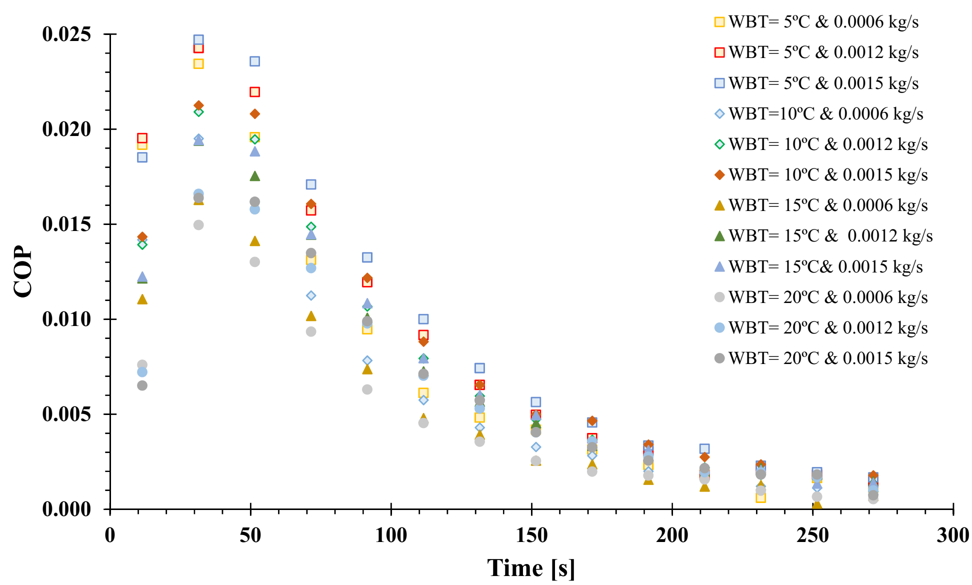

Fig. 12 COP results during cooling time for nanofluid Fe_3O_4–water (1.0% vol.) at different water bath temperatures and flow rates

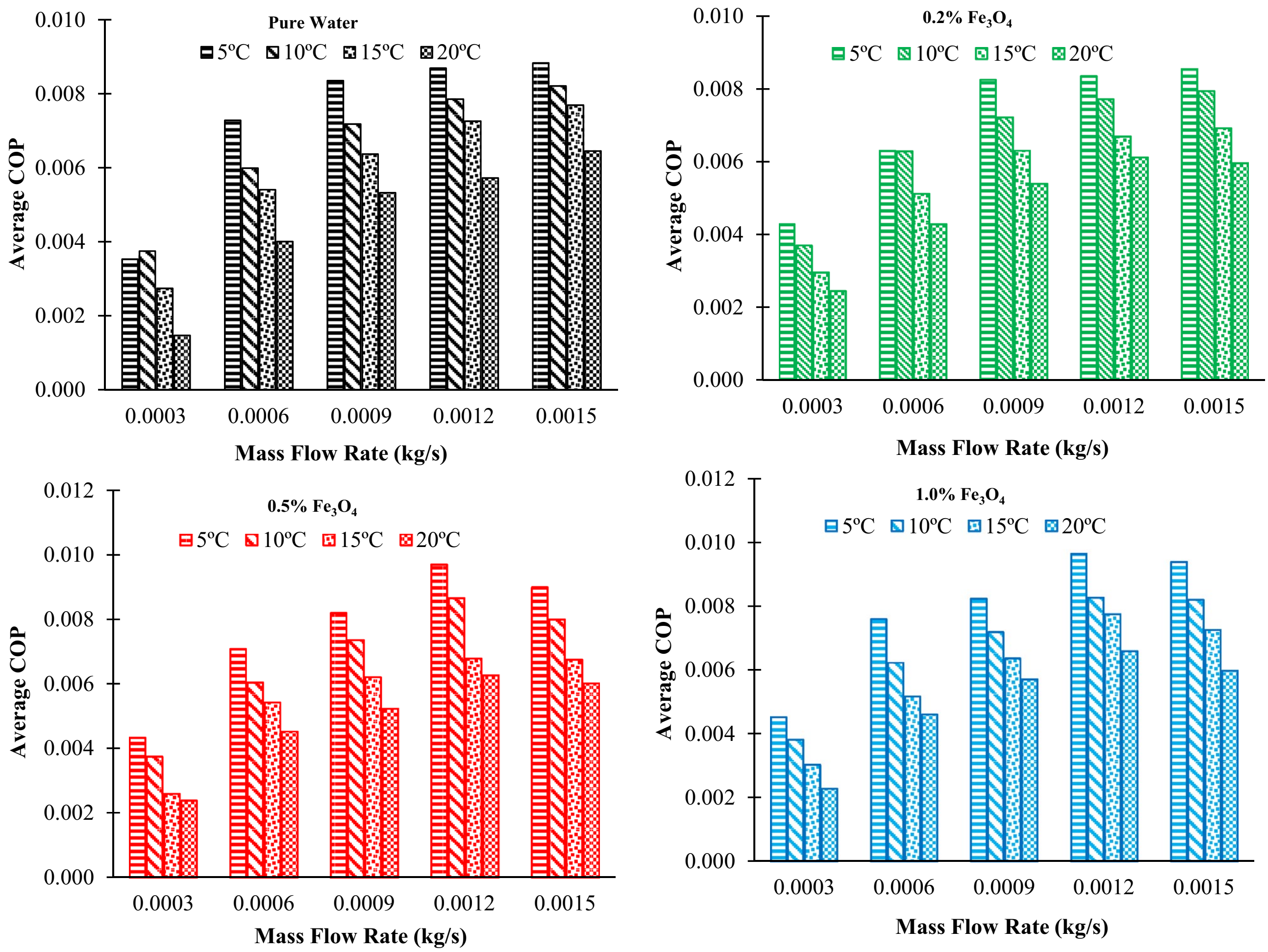

Fig. 13 Average COP results for all tested nanofluids at different water bath temperatures and flow rates

obtained using 1% vol. nanofluid instead of pure water. This rate grew to around 50% for the same water bath temperature and flow rate of 0.0003 kg/s. And also with the use of 1% vol. nanofluid, the COP increase was between 5 and 30% for a bath temperature of 5 ℃.

The physical reason for the increase in COP observed as a result of the usage of nanofluids is directly related to the increase in thermal conductivity. The use of nanofluids with a high thermal conductivity as the working fluid allows the thermoelectric cooler to remove waste heat more effectively. In this way, the surface temperature of the Peltier unit decreases, and its efficiency increases. The reason for this is the low thermal resistance obtained in the heat transfer zone. In addition, the particles in the nanofluid form additional micro-convection zones due to the Brownian Effect mechanism. This situation leads to the strengthening of convection interactions in the region where the waste heat will be removed.

5.2 Numerical results

In this work, CFD simulation of the used spiral heat exchanger has been performed. Generally, heat exchangers have many applications despite their relatively simple structure and play a very important role in energy systems (Jamshed et al. 2021; Gürbüz et al. 2020; Khanlari 2020; Selimefendigil and Şirin 2022; Khanlari et al. 2020). In this study, a cooling system was manufactured and a spiral-type heat exchanger was designed and employed in the system to cool the heat transfer fluid by heat transfer from the system to the water bath as explained previously. The used spiral heat exchanger plays an important role in cooling the heat transfer fluid, which is at a high temperature due to the extraction of heat energy from inside the cooling chamber by the Peltier module. For this reason, this element was considered to be simulated using ANSYS-Fluent and temperature distribution and flow structure were evaluated in the presented contours. In the CFD simulation, thermo-physical properties of nanofluid Fe_3O_4–water 0.2% vol., were defined to evaluate significant contours of the nanofluid as heat transfer fluid. First of all, the temperature volume rendering result of the heat exchanger has been presented in Fig. 14 to visualize obtained results in three-dimensional appearance. It can be stated that 3-D results can be analyzed for a better estimation of energy and flow conditions in the model.

In this section, the results of temperature and velocity are presented comparatively and the effects of different operating conditions on the contours are discussed. Due to the spiral form, presenting the results in 2D was difficult, but this problem was solved by choosing the proper plan in domain using a combination of 2D and 3D results to analyze the obtained results. As shown in Fig. 15, temperature distribution in spiral heat exchanger has been presented at different flow rates as 0.0003 kg/s, 0.0006 kg/s, 0.0009 kg/s, 0.0012 kg/s, and 0.0015 kg/s. Cooling water bath is kept at 278 K. At very low flow rates (Fig. 15a), it can be seen that, the fluid inside spiral exchanger has time enough to cool down by heat transfer to the water bath. However, as the flow

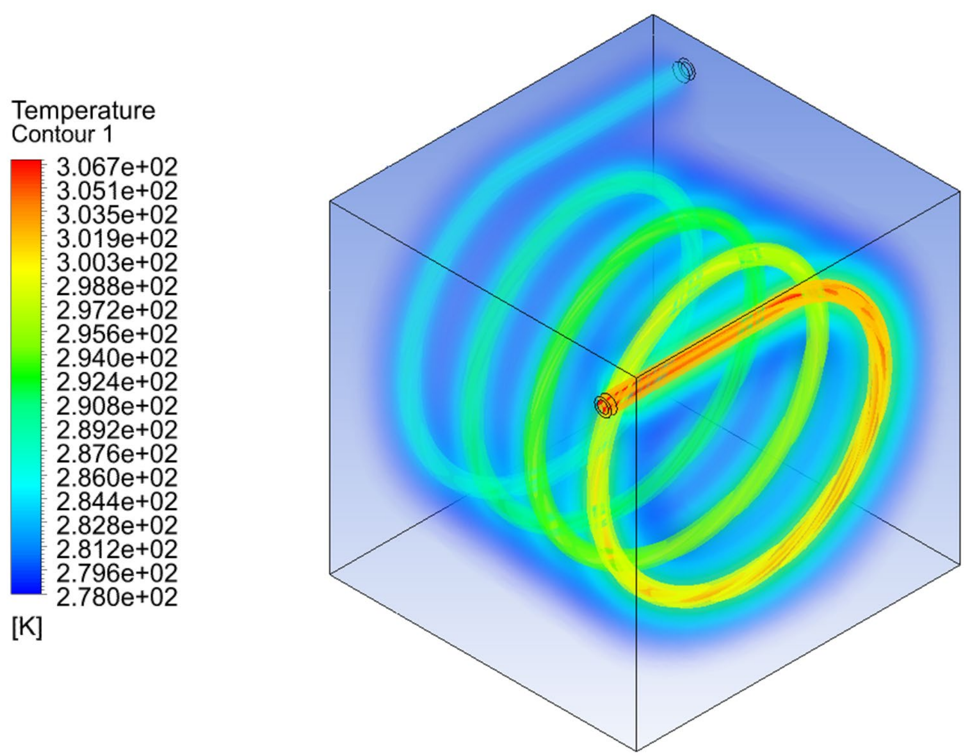

Fig. 14 Temperature volume rendering result of spiral heat exchanger

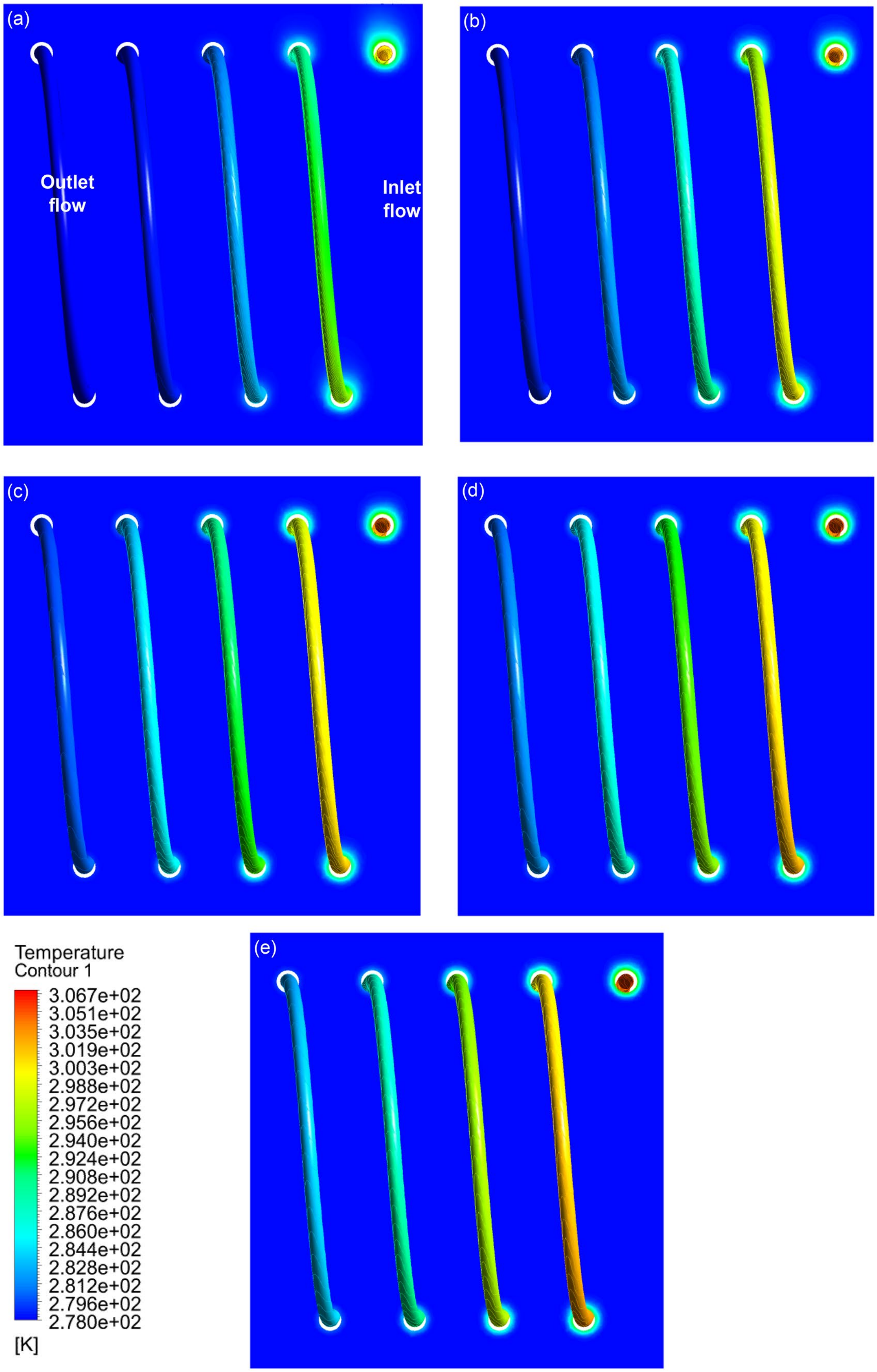

Fig. 15 Temperature contours in different flow rates 0.0003 kg/s (**a**), 0.0006 kg/s (**b**), 0.0009 kg/s (**c**), 0.0012 kg/s (**d**), and 0.0015 kg/s (**e**)

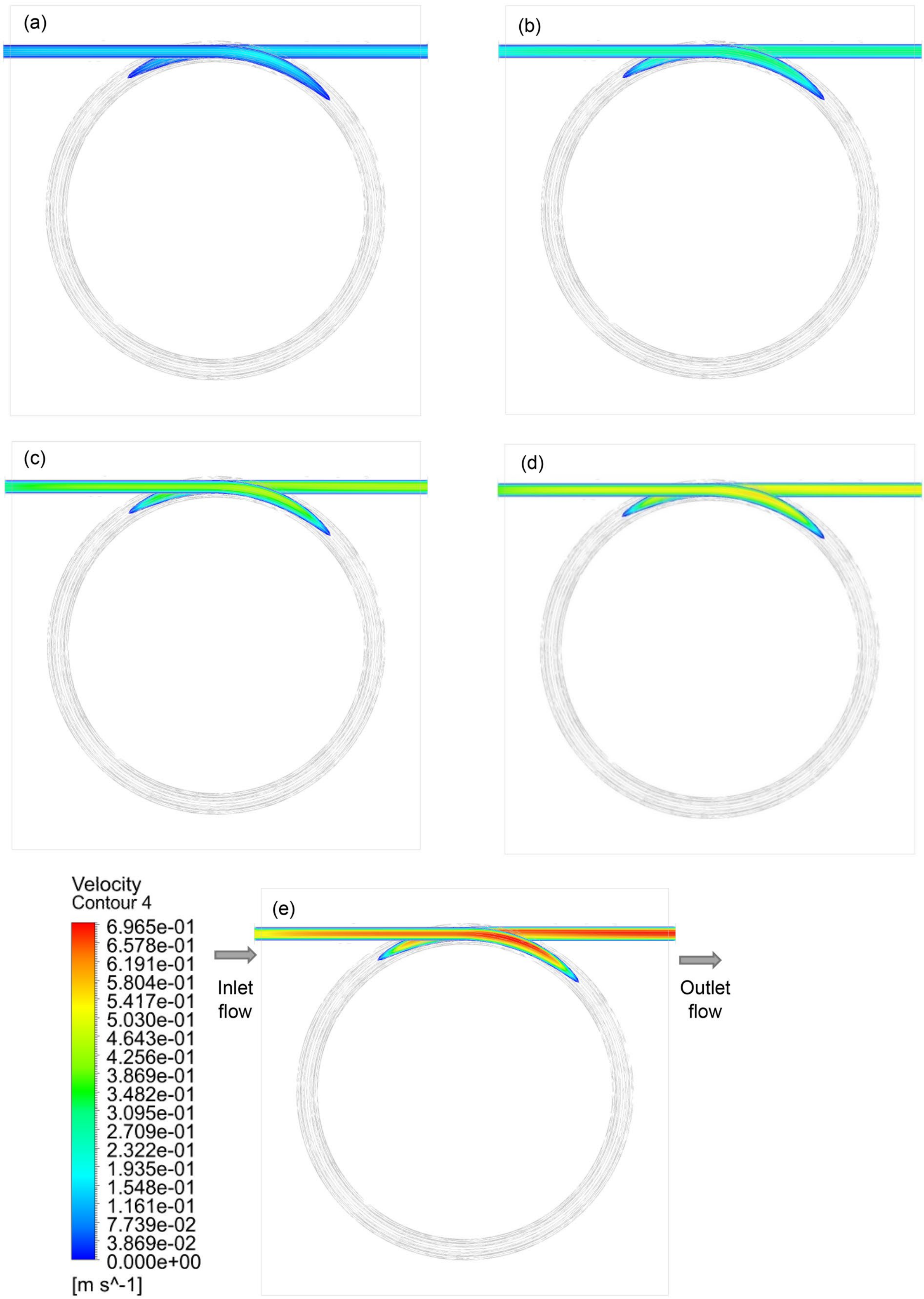

Fig. 16 Velocity contours in different flow rates 0.0003 kg/s (**a**), 0.0006 kg/s (**b**), 0.0009 kg/s (**c**), 0.0012 kg/s (**d**), and 0.0015 kg/s (**e**)

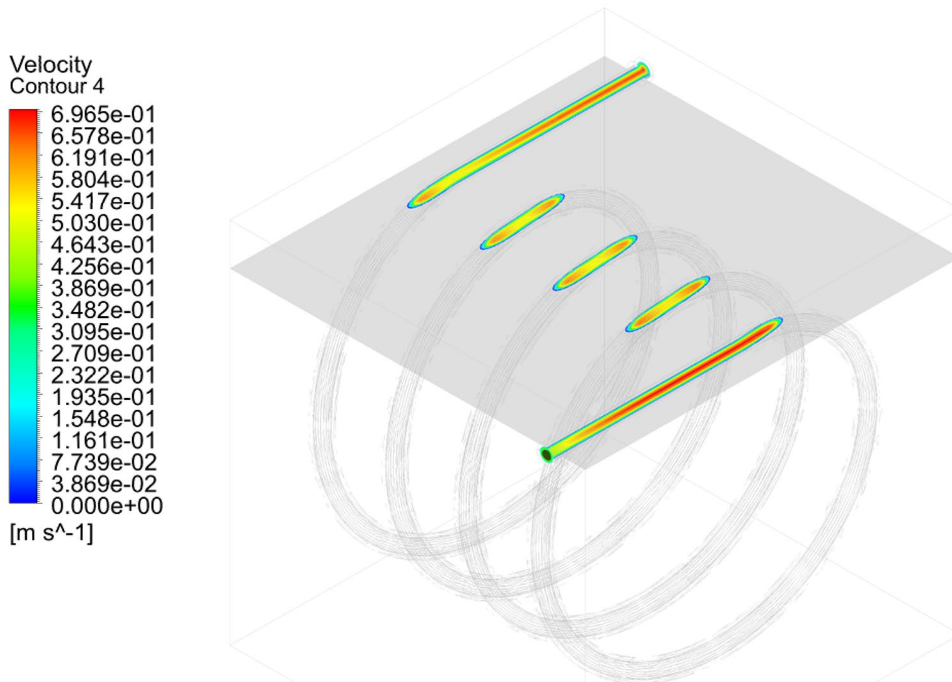

Fig. 17 Velocity contour on a plan on upper section of the spiral heat exchanger at 0.0015 kg/s

Table 3 Comparison of performance (COP) results in this study with literature (Ceviz et al. 2022)

References	Cooler class	Application	Performance
Gürbüz et al. (2022)	Diffusion absorption	Cooling apparatus	0.08–0.2
Sözen et al. (2021)	Diffusion absorption	Cooling apparatus	0.1
De Marchi et al. (2009)	Vapor compression cooling cycle	Conventional refrigerator	0.2–0.8
Min et al. (2006)	Thermoelectric	Prototype domestic refrigerator	0.36–1.1
Abdul-Wahab et al. (2009)	Thermoelectric	Portable solar TE refrigerator	0.16
Wang et al. (2011)	Organic Rankine cycle and vapor compression cycle combined	Integrated cycle	0.6
Martinez et al. (2013)	Thermoelectric	Refrigerator	0.14
Martinez et al. (2016)	Thermoelectric	Refrigerator	0.09–0.33
Mirmanto et al. (2019)	Thermoelectric	Cooling box	< 0.03
Afshari et al. (2022b)	Thermoelectric	TE refrigerator	0.01
Presented study	Thermoelectric	TE refrigerator	< 0.01

rate increases, the conditions change and the fluid inside the spiral exchanger has a reduced opportunity to heat transfer and the temperature is at higher levels. It can be noted that, the temperature of the fluid flowing in the last stages of the heat exchanger approximates the temperature of the water bath.

In Fig. 16, velocity contours of the spiral heat exchanger have been illustrated at the same flow rates. The flow rate inside the exchanger clearly shows that, as the mass flow rate increases, the velocity contour changes and the heat transfer fluid passes through the spiral exchanger more quickly. In the areas close to the walls, the velocity values are low and approach zero, which is a sign of friction and obstruction against the movement of the fluid inside heat exchanger.

In order to show the velocity scales and flow structure inside the tube, a plate was considered at the top of the spiral heat exchanger, and the velocity changes are demonstrated as shown in Fig. 17. This contour was provided for the case when mass flow rate is 0.0015 kg/s.

In Table 3, a comparison of COP results in this study with literature has been carried out. It can be seen that, in refrigerators, COP value is significantly lower and the results obtained in the present study are similar to the literature.

6 Conclusion

Peltier cooling systems have a relatively low efficiency despite their high potential for use in heating and cooling systems. In this study, an attempt has been made to improve their efficiency considering different parameters. Due to the fact that the deposition of nanoparticles is a major problem, the synthesized nanoparticles Fe_3O_4 were chemically modified for use in the present study. After stability analyses, water–(Fe_3O_4@SiO_2@$(CH_2)_3$IM) nanofluid was selected to be utilized as heat transfer fluid in the Peltier cooling system and the effect of fluid flow rate and fluid temperature was tested. This study revealed that, in Peltier cooling system, the effect of temperature and flow rate of heat transfer fluid is relatively greater. However, the choice of nanofluid can have a moderate improvement on system performance. Nanofluids were prepared in three different volume percentages of 0.2, 0.5, and 1% vol. and examined in different working conditions. This study was evaluated both experimentally and numerically using CFD method. The main heat exchanger of the system was simulated and temperature and flow structure inside spiral heat exchanger were analyzed. According to the obtained results, for the nanofluid sample Fe_3O_4–water (1.0% vol.), increasing the mass flow rate from 0.0003 kg/s to 0.0015 kg/s caused an increase in the average COP by about 150%. Additionally, at a water bath temperature of 5 °C, the temperature drops of the cooling chamber for pure water and nanofluid Fe_3O_4–water 0.5% vol. were compared, which indicates an improvement of about 1 °C using the nanofluid.

Acknowledgements This study has been supported by the Scientific and Technological Research Council of Turkey (TÜBİTAK, Project No. 119N727) and University of Tabriz and Iran Ministry of Science, Research and Technology (MSRT, Project No. 99-24-800). The authors gratefully acknowledge the support of this study.

Data availability The data that support the findings of this study are available from the corresponding author upon reasonable request.

Declarations

Conflict of interest The authors declare that they have no conflict of interest.

References

Abdul-Wahab SA, Elkamel A, Al-Damkhi AM, Is'haq A, Al-Rubai'ey HS, Al-Battashi AK, Chutani MU (2009) Design and experimental investigation of portable solar thermoelectric refrigerator. Renew Energy 34(1):30–34

Afshari F (2020) Experimental study for comparing heating and cooling performance of thermoelectric Peltier. Politeknik Dergisi 23(3):889–894

Afshari F (2021) Experimental and numerical investigation on thermoelectric coolers for comparing air-to-water to air-to-air refrigerators. J Therm Anal Calorim 144(3):855–868

Afshari F, Afshari F, Ceylan M, Ceviz MA (2020) A review study on peltier cooling devices; applications and performance. In Proceedings on 3nd International Conference on Technology and Science.

Afshari F, Ceviz MA, Manay E, Ceylan M, Muratçobanoğlu B (2022a) Performance analysis of air-to-water binary thermoelectric peltier cooling systems and determination of optimum arrangement. J Braz Soc Mech Sci Eng 44(9):424

Afshari F, Ceviz MA, Mandev E, Yıldız F (2022b) Effect of heat exchanger Base thickness and cooling fan on cooling performance of air-to-air thermoelectric refrigerator; experimental and numerical study. Sustain Energy Technol Assess 52:102178

Agwu Nnanna AG, Rutherford W, Elomar W, Sankowski B (2009) Assessment of Thermoelectric Module with Nanofluid Heat Exchanger. Appl Therm Eng 29(2–3):491–500

Ahammed N, Asirvatham LG, Wongwises S (2016a) thermoelectric cooling of electronic devices with nanofluid in a multiport minichannel heat exchanger. Exp Thermal Fluid Sci 74:81–90

Ahammed N, Asirvatham LG, Wongwises S (2016b) Entropy generation analysis of graphene-alumina hybrid nanofluid in multiport minichannel heat exchanger coupled with thermoelectric cooler. Int J Heat Mass Transf 103:1084–1097

Asadollahi A, Esfahani JA, Ellahi R (2019) Evacuating liquid coatings from a diffusive oblique fin in micro-/mini-channels: an application of condensation cooling process. J Therm Anal Calorim 138(1):255–263

Bhatti MM, Sait SM, Ellahi R (2022) Magnetic nanoparticles for drug delivery through tapered stenosed artery with blood based non-newtonian fluid. Pharmaceuticals 15(11):1352

Buonomo B, Manca O, Marinelli L, Nardini S (2015) Effect of temperature and sonication time on nanofluid thermal conductivity measurements by nano-flash method. Appl Therm Eng 91:181–190

Çağlar A (2018) Optimization of operational conditions for a thermoelectric refrigerator and its performance analysis at optimum conditions. Int J Refrig 96:70–77

Ceviz MA, Afshari F, Muratçobanoğlu B, Ceylan M, Manay E (2022) Computational fluid dynamics simulation and experimental investigation of a thermoelectric system for predicting influence of applied voltage and cooling water on cooling performance. Int J Numer Meth Heat Fluid Flow 33(1):241–262

Chein R, Chen Y (2005) Performances of thermoelectric cooler integrated with microchannel heat sinks. Int J Refrig 28(6):828–839

Çiftçi E, Khanlari A, Sözen A, Aytaç İ, Tuncer AD (2021) Energy and exergy analysis of a photovoltaic thermal (PVT) system used in solar dryer: a numerical and experimental investigation. Renewable Energy 180:410–423

Cosnier M, Fraisse G, Luo L (2008) An experimental and numerical study of a thermoelectric air-cooling and air-heating system. Int J Refrig 31(6):1051–1062

Cuce E, Guclu T, Cuce PM (2020) Improving thermal performance of thermoelectric coolers (TECs) through a nanofluid driven water to air heat exchanger design: an experimental research. Energy Convers Manage 214:112893

De Marchi Neto I, Padilha A, Scalon VL (2009) Refrigerator COP with thermal Storage. Appl Therm Eng 29(11–12):2358–2364

Ellahi R (2013) The effects of MHD and temperature dependent viscosity on the flow of non-Newtonian nanofluid in a pipe: analytical solutions. Appl Math Model 37(3):1451–1467

Esfe MH, Afrand M, Karimipour A, Yan WM, Sina N (2015) An experimental study on thermal conductivity of MgO nanoparticles suspended in a binary mixture of water and ethylene glycol. Int Commun Heat Mass Transfer 67:173–175

Fatchurrohman N, Chia ST (2017) Performance of hybrid nano-micro reinforced mg metal matrix composites brake calliper: simulation approach. IOP Conf Series Mater Sci Eng 257(1):012060

Gökçek M, Şahin F (2017) Experimental performance investigation of minichannel water cooled-thermoelectric refrigerator. Case Stud Therm Eng 10:54–62

Güngör A, Khanlari A, Sözen A, Variyenli HI (2022) Numerical and experimental study on thermal performance of a novel shell and helically coiled tube heat exchanger design with integrated rings and discs. Int J Therm Sci 182:107781

Gupta N, Gupta SM, Sharma SK (2021) Synthesis, characterization and dispersion stability of water-based Cu–CNT hybrid nanofluid without surfactant. Microfluid Nanofluid 25:1–14

Gürbüz EY, Sözen A, Variyenli Hİ, Khanlari A, Tuncer AD (2020) A comparative study on utilizing hybrid-type nanofluid in plate heat exchangers with different number of plates. J Braz Soc Mech Sci Eng 42(10):1–13

Gürbüz EY, Sözen A, Keçebaş A, Özbaş E (2022) Experimental and numerical investigation of diffusion absorption refrigeration system working with ZnO, Al_2O_3 and TiO_2 nanoparticles added ammonia/water nanofluid. Exp Heat Transf 35(3):197–222

He Y, Li R, Fan Y, Zheng Y, Chen G (2021) Study on the performance of a solid-state thermoelectric refrigeration system equipped with ionic wind fans for ultra-quiet operation. Int J Refrig 130:441–451

Huminic G, Huminic A (2011) Heat transfer characteristics in double tube helical heat exchangers using nanofluids. Int J Heat Mass Transf 54(19–20):4280–4287

Jamshed W, Şirin C, Selimefendigil F, Shamshuddin MD, Altowairqi Y, Eid MR (2021) Thermal characterization of coolant Maxwell type nanofluid flowing in parabolic trough solar collector (PTSC) used inside solar powered ship application. Coatings 11(12):1552

Khanlari A (2020) The effect of utilizing Al_2O_3-SiO_2/Deionized Water hybrid Nanofluid in A Tube-type Heat Exchanger. Heat Transfer Res 51(11):991–1005

Khanlari A, Yılmaz Aydın D, Sözen A, Gürü M, Variyenli Hİ (2020) Investigation of the influences of Kaolin-Deionized water nanofluid on the thermal behavior of concentric type heat exchanger. Heat Mass Transf 56(5):1453–1462

Kumar N, Sonawane SS (2016) Experimental study of Fe_2O_3/water and Fe_2O_3/ethylene glycol nanofluid heat transfer enhancement in a shell and tube heat exchanger. Int Commun Heat Mass Transf 78:277–284

Lin X, Mo S, Mo B, Jia L, Chen Y, Cheng Z (2020) Thermal management of high-power LED based on thermoelectric cooler and nanofluid-cooled microchannel heat sink. Appl Therm Eng 172:115165

Liu Y, Liu Y, Hu P, Li X, Gao R, Peng Q, Wei L (2015) The effects of graphene oxide nanosheets and ultrasonic oscillation on the supercooling and nucleation behavior of nanofluids PCMs. Microfluid Nanofluid 18:81–89

Mandev E, Manay E, Rahimpour S, Mohammadzadeh A, Sahin B, Afshari F, Teimuri-Mofrad R (2022) Surface modification of Fe_3O_4 nanoparticles for preparing stable water-based nanofluids. Heat Transf Res 53(18):39–55

Maneewan S, Thongtha A, Punlek C (2014) Coefficient of performance of thermoelectric cooling on nanofluids. Appl Mech Mater 459:91–99

Martinez A, Astrain D, Rodríguez A, Pérez G (2013) Reduction in the electric power consumption of a thermoelectric refrigerator by experimental optimization of the temperature controller. J Electron Mater 42(7):1499–1503

Martinez A, Astrain D, Rodriguez A, Aranguren P (2016) Advanced computational model for Peltier effect-based refrigerators. Appl Therm Eng 95:339–347

Min G, Rowe DM (2006) Experimental evaluation of prototype thermoelectric domestic-refrigerators. Appl Energy 83(2):133–152

Mirmanto M, Syahrul S, Wirdan Y (2019) Experimental performances of a thermoelectric cooler box with thermoelectric position variations. Eng Sci Technol Int J 22(1):177–184

Mohammadian SK, Zhang Y (2014) Analysis of nanofluid effects on thermoelectric cooling by micro-pin-fin heat exchangers. Appl Therm Eng 70(1):282–290

Nguyen CT, Roy G, Gauthier C, Galanis N (2007) Heat transfer enhancement using Al_2O_3–water nanofluid for an electronic liquid cooling system. Appl Therm Eng 27(8–9):1501–1506

Özerinç S, Kakaç S, Yazıcıoğlu AG (2010) Enhanced thermal conductivity of nanofluids: a state-of-the-art review. Microfluid Nanofluid 8:145–170

Park H, Lee J, Lim J, Cho H, Kim J (2022) Optimal operating strategy of ash deposit removal system to maximize boiler efficiency using CFD and a thermal transfer efficiency model. J Ind Eng Chem 110:301–317

Pourkiaei SM, Ahmadi MH, Sadeghzadeh M, Moosavi S, Pourfayaz F, Chen L, Kumar R (2019) Thermoelectric cooler and thermoelectric generator devices: a review of present and potential applications. Model Mater Energy 186:115849

Putra N, Iskandar FN (2011) Application of nanofluids to a heat pipe liquid-block and the thermoelectric cooling of electronic equipment. Exp Thermal Fluid Sci 35(7):1274–1281

Rahman Salari S, Khavarpour M, Masoumi M, Mosivand S (2022) Preparation of cobalt oxide and tin dioxide nanofluids and investigation of their thermophysical properties. Microfluid Nanofluid 26(10):79

Sadeghi R, Etemad SG, Keshavarzi E, Haghshenasfard M (2015) Investigation of alumina nanofluid stability by UV–Vis spectrum. Microfluid Nanofluid 18:1023–1030

Selimefendigil F, Şirin C (2022) Experimental investigation of a parabolic greenhouse dryer improved with copper oxide nano-enhanced latent heat thermal energy storage unit. Int J Energy Res 46(3):3647–3662

Selimefendigil F, Şirin C, Öztop HF (2021) Effect of different heat transfer fluids on discharging performance of phase change material included cylindrical container during forced convection. J Central South Univ 28(11):3521–3533

Sözen A, Keçebaş A, Gürbüz EY (2021) Enhancing the thermal performance of diffusion absorption refrigeration system by using magnesium aluminate spinel oxide compound nanoparticles: an experimental investigation. Heat Mass Transf 57(10):1583–1592

Tan G, Zhao D (2015) Study of a thermoelectric space cooling system integrated with phase change material. Appl Therm Eng 86:187–198

Teimuri-Mofrad R, Esmati S, Tahmasebi S, Gholamhosseini-Nazari M (2018a) Bisferrocene-containing ionic liquid supported on silica coated Fe_3O_4: a novel nanomagnetic catalyst for the synthesis of dihydropyrano [2, 3-c] coumarin derivatives. J Organomet Chem 870:38–50

Teimuri-Mofrad R, Ahadzadeh I, Gholamhosseini-Nazari M, Esmati S, Shahrisa A (2018b) Synthesis of betti base derivatives catalyzed by nano-CuO-ionic liquid and experimental and quantum chemical studies on corrosion inhibition performance of them. Res Chem Intermed 44(4):2913–2927

Tiwari AK, Ghosh P, Sarkar J (2013) Performance comparison of the plate heat exchanger using different nanofluids. Exp Thermal Fluid Sci 49:141–151

Tuncer AD, Sözen A, Khanlari A, Amini A, Şirin C (2020) Thermal performance analysis of a quadruple-pass solar air collector assisted pilot-scale greenhouse dryer. Sol Energy 203:304–316

Tuncer AD, Sözen A, Khanlari A, Gürbüz EY, Variyenli Hİ (2021) Upgrading the performance of a new shell and helically coiled heat exchanger by using longitudinal fins. Appl Therm Eng 191:116876

Wang H, Peterson R, Herron T (2011) Design study of configurations on system COP for a combined ORC (organic Rankine cycle) and VCC (vapor compression cycle). Energy 36(8):4809–4820

Wiriyasart S, Suksusron P, Hommalee C, Siricharoenpanich A, Naphon P (2021) Heat transfer enhancement of thermoelectric cooling module with nanofluid and ferrofluid as base fluids. Case Stud Therm Eng 24:100877

Xuan Y, Roetzel W (2000) Conceptions for heat transfer correlation of nanofluids. Int J Heat Mass Transf 43(19):3701–3707

Yu W, France DM, Routbort JL, Choi SU (2008) Review and comparison of nanofluid thermal conductivity and heat transfer enhancements. Heat Transfer Eng 29(5):432–460

Zeeshan A, Shehzad N, Atif M, Ellahi R, Sait SM (2022) Electromagnetic flow of SWCNT/MWCNT suspensions in two immiscible water- and engine-oil-based newtonian fluids through porous media. Symmetry 14(2):406

Zheng D, Wang J, Chen Z, Baleta J, Sundén B (2020) Performance analysis of a plate heat exchanger using various nanofluids. Int J Heat Mass Transf 158:119993